

# Finding Survivable Routes in Multi-domain Optical Networks with Geographically Correlated Failures [Invited]

Riti Gour, *Student Member, IEEE*, Jian Kong, *Student Member, IEEE*, Genya Ishigaki, *Student Member, IEEE*, Ashkan Yousefpour, *Student Member, IEEE*, Sangjin Hong, *Member, IEEE*, and Jason P. Jue, *Senior Member, IEEE*

**Abstract**—This work presents the problem of survivable path pair routing in multi-domain optical networks with geographically correlated failures. The objective is to minimize the risk of simultaneous failure of both the primary and backup paths. We develop a probabilistic model to calculate the simultaneous failure probability of both the paths under circular geographic failures with uniform and non-uniform distributions of epicenter location. We develop topology aggregation techniques and an inter-domain minimum overlapping area routing algorithm based on the aggregated information from each domain. Our algorithm is compared to Suurballe’s Algorithm (SUR) and an approach with full information shared amongst domains, and we show that our heuristic approach is effective in reducing the total probability of simultaneous failure.

**Index Terms**—Multi-domain optical network, survivability, geographically correlated failures, topology aggregation.

## I. INTRODUCTION

OPTICAL networks may be prone to geographically correlated failures, which not only affect components at the epicenter of the failure, but which may also lead to the failure of neighboring network components, resulting in a tremendous amount of information loss. For example, an earthquake in Nepal in 2015 knocked out thousands of network components due to technical failure. Other examples of events that lead to geographically correlated failures are manmade disasters, such as EMP (electromagnetic pulse) attacks and nuclear attacks [2]. Considering such geographically correlated failures, it is important to protect the ability of the network to continue carrying traffic when such failures occur by developing appropriate survivability mechanisms.

The probability of physical failure for the network components typically depends on both the geographical distance of the components to the center of the failure event and the intensity of the disaster. In order to understand the occurrence of some failure events in a specific geographical region, the correlation of the event with the probability of occurrence of other events in the vicinity should be considered. For example,

Manuscript received February 20, 2018, revised May 16, 2018.

Riti Gour, Jian Kong, Genya Ishigaki, Ashkan Yousefpour and Jason P. Jue are with Erik Jonsson School of Engineering and Computer Science, The University of Texas at Dallas, Richardson, TX, 75080 USA (E-mail: rgour@utdallas.edu).

Sangjin Hong is with the Department of Computer Science, Saint Leo University, St Leo, Florida 33574, USA.

An earlier version of this work appeared in GLOBECOM 2017, Singapore [1].

earthquakes may trigger other earthquakes and aftershocks in their surrounding, representing a correlation between epicenters [3].

A common approach to providing survivability at the network layer is to provision protection resources in the network [4]. In path protection schemes, for each working path, a link-disjoint backup path is provisioned in order to protect against the failure of any link along the working path. However, under correlated failures, such an approach may not be effective if links on the primary path share correlated risks with links on the backup path. One approach to deal with correlated failures is through the concept of shared risk link groups (SRLGs), in which each SRLG identifies a set of links that fail simultaneously due to the same risk. In this case, survivability can be provided by provisioning an SRLG-disjoint backup path for each working path. However, the problem of finding SRLG-disjoint paths has been shown to be NP-complete [5]. Furthermore, for the case of geographically correlated failures in which the location of the epicenter of the failure is not known in advance, it may be difficult and impractical to model all possible failure events using SRLGs.

Additionally, providing survivability in a multi-domain environment is an even greater challenge than in single-domain environments because full information regarding the resources in each domain is often not available due to the privacy policies of domain administrators [6]–[9]. One technique for facilitating path provisioning over multi-domain optical networks is topology aggregation, which is used for exchanging limited domain information while maintaining the privacy of domain administrators [8]. In topology aggregation, each domain is represented by an aggregated logical topology in which aggregated links interconnect the border nodes of the domain. The underlying intra-domain paths for the aggregated links are not revealed to other domains. The aggregated topology may also provide some limited information for each of the aggregated links, and the amount of information to be exchanged could depend upon domain policies. In some cases, only the distance of the shortest paths between border nodes is presented in topology aggregation, while some other aggregations might provide information on the disjointness of aggregated links through SRLGs [7].

This paper considers the problem of finding a pair of paths (primary and backup) in a multi-domain optical network, such that the probability of simultaneous failure of both the primary

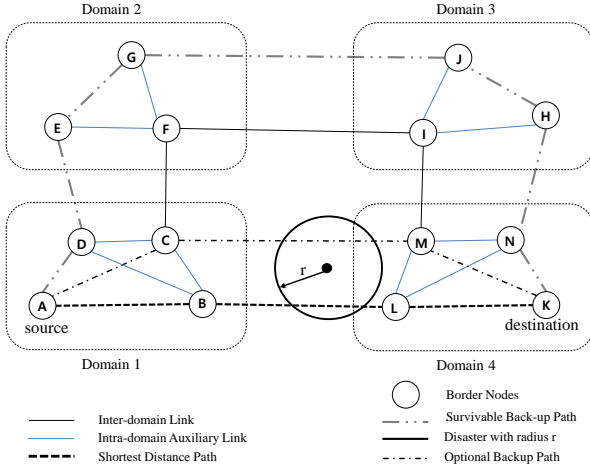


Fig. 1. Survivable routing scheme against a random disk-shaped geographically correlated failure with radius  $r$ .

path and backup path is minimized. In our preceding work [1], we consider a geographically correlated failure model in which a failure is represented by a circular disk, located uniformly in the plane of the network with an assumption that all components within the area of this circular disk fail simultaneously. In this paper, we extend our model to a non-uniform distribution of failure event epicenter location in the network plane. Furthermore, the intractability of this problem is evaluated by reduction to the Region Disjoint Paths Problem. We propose a topology aggregation scheme for each domain that provides necessary information about the geographic distances between links in the domain. Then, using this aggregated topology information, we develop a heuristic algorithm to provision primary and backup paths in such a way that they are less likely to fail simultaneously due to a geographically correlated failure. To motivate our survivability constraint mentioned in the first statement, we include an example in the next section.

### A. An Example

Fig. 1 shows a scenario of a multi-domain network with four domains. A circle with radius  $r$  shows the geographical failure and the network components that are affected by the geographical failure. Consider three routing paths from source  $A$  to destination  $K$ . In this example, if our primary path is  $A-B-L-K$  (considering shortest distance path from source to destination) and it fails, then path  $A-C-M-K$  cannot be used as a backup path, since it lies in the same disaster region as the primary path. On the other hand, path  $A-D-E-G-J-H-N-K$  is far enough from the primary path that it is less likely to fail at the same time, and thus could be a possible choice of backup.

### B. Related Works

Survivability in multi-domain optical networks has been a well-researched area. In [9], the authors survey survivability techniques in multi-domain optical networks and compare

the performances of different approaches based on different metrics. Most of these works focus on either a single component failure or a small number of simultaneous fiber cuts. Correlated failures of nodes and links can be often addressed by the concept of shared risk node groups or SRLGs [10]. In [7], Gao et al. propose SRLG-aware topology aggregation approaches that can help to find a pair of inter-domain paths with a minimum set of common SRLGs for multi domain optical networks. In [11], the authors present a protection scheme for multi-domain optical networks for correlated and probabilistic failures using a p-SRLG framework for multi-domain networks.

The problem of survivability of networks against geographically correlated failures has been extensively studied in works such as [2], [3], [12]–[14]. The work in [2] includes the use of computational geometric tools to construct algorithms that identify vulnerable points within the network under various metrics. [12] presents a survey of strategies for protection against geographically correlated failures or large scale disasters. In [13], the authors consider disasters that take the form of random line cuts and emphasize geometric techniques to evaluate average two-terminal reliability towards the study of network resiliency. In [14] the authors study disasters as randomly located disks in the network plane, and using results from geometric probability, they approximate some network performance metrics to such a disaster in polynomial time. [3] presents a stochastic model, based on spatial point processes, for representing epicenters on the network plane in order to model spatially inhomogeneous and correlated link failures in communication networks. Different scenarios with inhibition or clustering between epicenters are presented, which enables detailed assessment of vulnerabilities of the network to the level of inhomogeneity and spatial correlation. Although these papers discuss the impacts of geographical failures, they consider networks as single domain architectures. The additional challenge in providing survivability in multi-domain networks with geographically correlated failures is to develop a topology aggregation scheme that provides necessary information about the topological locations of nodes and edges within a domain.

The rest of the paper is structured as follows. Section II presents the problem statement, description of the network model and failure model, and a probabilistic model to calculate the simultaneous failure probability for two paths. Section III presents details of the topology aggregation scheme, and discusses the algorithm for finding a pair of survivable multi-domain paths based on the topology aggregations. In Section IV, we present the numerical evaluation of our algorithm, comparing it to Suurballe’s algorithm and a full information approach for calculating region disjoint paths. Discussions are provided in Section V. We conclude our paper in Section VI.

## II. PROBLEM STATEMENT AND FAILURE MODELING

We begin this section by describing our multi-domain network model, followed by the failure model, and then we introduce the concept of vulnerable zone of edges and paths. We also discuss a probabilistic model to calculate simultaneous failure probability for two paths, first under assumption

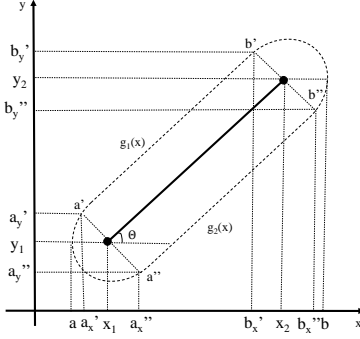


Fig. 2. Geometrical representation for vulnerable zones around an edge.

that the failure location is uniformly distributed in the plane of the network and then extend it to non-uniform distribution of the failure location.

A physical multi-domain network is denoted by a graph  $G_p (D_p, L_p, C_p)$ , where  $D_p$  is a set of domains,  $L_p$  is a set of bi-directional inter-domain links and  $C_p: L_p \rightarrow \mathbb{R}_+$  is a set of inter-domain link distances. Domain  $i$  is denoted by graph  $G_i (V_i, E_i, B_i, C'_i)$ , where  $V_i$  is a set of intra-domain nodes for Domain  $i$ ,  $E_i$  is a set of bi-directional intra-domain links for Domain  $i$ ,  $B_i$  is a set of border nodes for Domain  $i$ , and  $C'_i: E_i \rightarrow \mathbb{R}_+$  is a set of intra-domain link distances within Domain  $i$ . We assume that inter-domain link distances are greater than intra-domain link distances. We are also given a set of physical coordinates,  $(X_v, Y_v)$ , that denotes the location of each node  $v \in V_i$  in the physical plane of the network. We assume all edge locations are straight lines between nodes in the physical plane of the network.

We model a geographically correlated failure as a circular region of radius  $r$  centered at a random location in the physical plane of the network. We assume that there is only one geographically correlated failure in the network at a time, and that all network components located within the area of the circular region of radius  $r$  will fail at the same time. The location of the epicenter of the failure is determined by a two-dimensional probability density function  $f(x, y)$  defined over the plane of the network.

In this paper, we assume that the physical locations in the network are mapped to a planar coordinate system. Alternatively, in large-scale long-haul networks, such as inter-continental networks, locations may be mapped to spherical coordinates on the Earth's surface. While projecting spherical coordinates to planar coordinates may introduce some distortion [15], the study of such distortions is beyond the scope of this paper.

### A. Probabilistic Model

Based on the failure model, we define the *vulnerable zone of an edge*,  $VZ_{e(i,j)}$ , as the region around edge  $e(i,j)$  in the network plane, such that if the epicenter of a failure is located within this region, it will cause failure of edge  $e(i,j)$  [2]. Figure 2 illustrates the concept of vulnerable zone around an edge. All points within  $VZ_{e(i,j)}$  are at a distance of less than  $r$  from edge  $e(i,j)$ . The failure probability ( $P_{f_{e(i,j)}}$ ) of an edge  $e(i,j)$

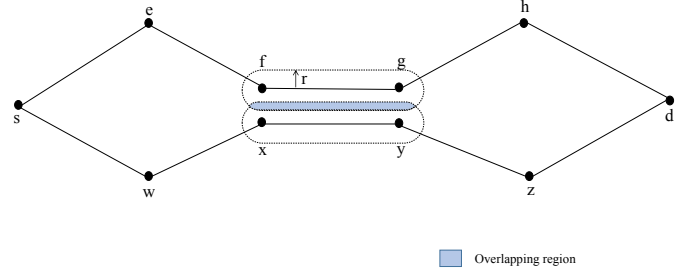


Fig. 3. Representation of the overlapping region of two paths between a pair of border nodes.

is determined by the probability that a failure occurs in the vulnerable zone of the edge.

The probability that the failure occurs in the vulnerable zone is determined by integrating the failure location probability density function  $f(x, y)$  over the vulnerable zone. In the case of uniform distribution of the failure's epicenter location, the probability is directly proportional to the area of the vulnerable zone itself. In general, the failure probability ( $P_{f_{e(i,j)}}$ ) of edge  $e(i,j)$  can be written as:

$$P_{f_{e(i,j)}} = \int_a^b \int_{g_2(x)}^{g_1(x)} f(x, y) dx dy, \quad (1)$$

where  $a$  and  $b$  are the leftmost and rightmost points of the vulnerable zone in the  $x$ - $y$  plane, and  $g_1(x)$  and  $g_2(x)$  are the curves denoting the upper and lower boundaries of the vulnerable zone (see Figure 2). For the case in which  $f(x, y)$  is uniform,  $P_{f_{e(i,j)}} = a_{12}/\Omega$ , where  $a_{12}$  is the area of the vulnerable zone, and  $\Omega$  is the area of the entire plane of the network. We define the vulnerable zone  $VZ_{R(s,d)}$  of a path  $R(s,d)$  from source node  $s$  to destination node  $d$  to be the union of vulnerable zones  $VZ_{e(i,j)}$  of all the edges  $e(i,j)$  in path  $R(s,d)$ .

$$VZ_{R(s,d)} = \bigcup_{e(i,j) \in R(s,d)} VZ_{e(i,j)}, \quad (2)$$

$$P_{f_{R(s,d)}} = \int_{VZ_{R(s,d)}} f(x, y) dx dy, \quad (3)$$

where  $P_{f_{R(s,d)}}$  is the probability of failure of path  $R(s,d)$ .

Let  $A(R(s,d), R(s',d'))$  be the overlapping region between the vulnerable zones of path  $R(s,d)$  and path  $R(s',d')$ :

$$A(R(s,d), R(s',d')) = VZ_{R(s,d)} \cap VZ_{R(s',d')}. \quad (4)$$

The probability of  $R(s,d)$  and  $R(s',d')$  failing simultaneously is then given by:

$$P_A = \int_{A(R(s,d), R(s',d'))} f(x, y) dx dy. \quad (5)$$

For the case in which the failure location is uniformly distributed, the probability of simultaneous failure is proportional to the area of the overlapping region of the two paths, which is denoted as  $\delta(R(s,d), R(s',d'))$ . One approach to calculate the area of the overlapping region,  $\delta(R(s,d), R(s',d'))$ , of two paths, is to overlay an  $N \times N$  grid over the plane of the network for a large value of  $N$ . Then consider  $K = N^2$  grid

points at the intersection of the grid lines, and for each of these grid points, if the distance between the grid point and the path  $R_{(s,d)}$  is less than  $r$ , then the grid point lies in the vulnerable zone  $VZ_{R_{(s,d)}}$ . Let  $K'$  be the number of grid points that fall within the vulnerable zone of both path  $R_{(s,d)}$  and  $R_{(s',d')}$ . The area of the overlapping region of the two paths (refer Figure 3) can then be estimated as  $(K'/K)$  multiplied by the area of the entire plane of the network,  $\Omega$ :

$$\delta(R_{(s,d)}, R_{(s',d')}) = (K'/K) \times \Omega, \quad (6)$$

and the probability of  $R_{(s,d)}$  and  $R_{(s',d')}$  failing simultaneously can be estimated as  $\frac{\delta(R_{(s,d)}, R_{(s',d')})}{\Omega}$ .

The area of the overlapping region,  $\delta(R_{(s,d)}, R_{(s',d')})$ , is used in the topology aggregation scheme to assist in finding pairs of paths through a domain that have minimum overlapping areas, which indicates that the paths are less susceptible to a common geographically correlated failure.

For the case in which the probability density function of the location of the epicenter is non-uniform, the probability density function may be obtained based on a hazard map generated from real data, as in Fig. 4 [16]. In such cases, the hazard map could be assumed as a collection of discrete grid points spread throughout the geographical space, in which points in the network plane may have various intensities, as shown by different colors. The probability density of the failure location can be obtained from the hazard map as follows:

$$f(x, y) = z \cdot c(x, y), \quad (7)$$

where,  $z$  is a normalization constant, and  $c(x, y)$  is the intensity of each point from the hazard map. To obtain the intensities from the given hazard map, we use the inbuilt tools in MATLAB R2017a and adjust the intensity values for the given map on a scale of 0 - 9. Then, the  $P_A$  is the volume under the height function  $f(x, y)$  over the overlapping area. Similarly in this case, we estimate the probability of simultaneous failure of the two paths as  $\gamma(R_{(s,d)}, R_{(s',d')})$ . Let  $\mathcal{G}$  be the set of  $(x, y)$  grid points in the vulnerable zone of both paths  $R_{(s,d)}$  and  $R_{(s',d')}$ , then:

$$\gamma(R_{(s,d)}, R_{(s',d')}) = \sum_{(x,y) \in \mathcal{G}} k \cdot f(x, y), \quad (8)$$

where,  $k$  is the area of small square around each grid point and is used for scaling. As  $\Omega$  is the area of the network plane, then  $L = \sqrt{\Omega}$  is the width of the plane (assuming a square plane). If we set an  $N \times N$  grid, then the area of the small square around each grid point is  $k = L/N \times L/N$ .

Given the above framework, the goal is to develop a topology aggregation scheme that takes into account the area of the overlapping region of two paths, and to use the information provided by the topology aggregation scheme to find two multi-domain paths from  $s$  to  $d$  such that the simultaneous failure probability of the two paths is minimized.

### B. Intractability

To prove the  $\mathcal{NP}$ -completeness of the *Minimum Overlapping Area Routing Problem* we select the *Region-Disjoint*

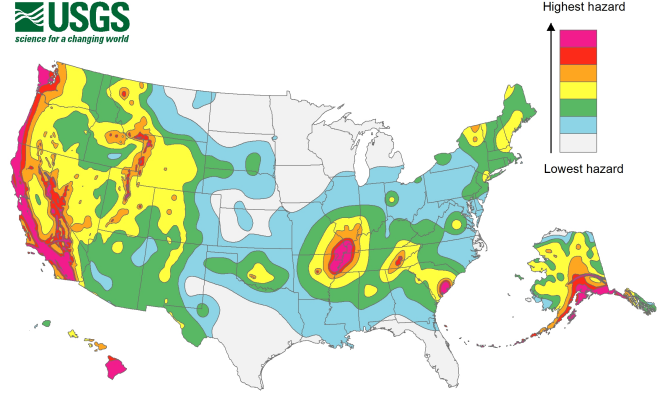


Fig. 4. Hazard map showing distribution of seismic hazards in 2014. [16]

*Paths Problem*, which is already proved to be  $\mathcal{NP}$ -complete using 3-SAT [17]. Formal descriptions of both problems are presented first, followed by the reduction of the *Minimum Overlapping Area Routing Problem* to a *decision problem*.

**Problem 1. Region-Disjoint Paths Problem:** Given a network  $G[V,E]$  with positive link weights and the diameter of a failure region (an arbitrary two-dimensional figure), find two region-disjoint paths from  $s$  to  $d$ , with a minimum total weight as reflected by the sum of the link weights in the two paths.

**Problem 2. Minimum Overlapping Area Routing Problem:** Given a multi-domain network  $G[V,E]$ , with positive link weights and given the diameter of an arbitrary two-dimensional circular disk, find two paths from  $s$  to  $d$  with minimum total weight. The weights of the two paths are denoted by a linear combination of non negative link distance and area of the overlapping region between them.

**Problem 3. Decision Problem:** Given a network  $G[V,E]$ , along with the radius of a two-dimensional circular disk, and the two paths from  $s$  to  $d$ , will the area of the overlapping region of the two paths be less than some value  $\mathcal{A}$  and will the link distance be less than some value  $\mathcal{D}$  (assuming a bound on the area of the overlapping region and the link distance)?

*Proof.* The process of finding the region disjoint paths in  $G[V,E]$  considers that the two paths will be completely node and link disjoint and are at least  $D = 2r$  distance apart from each other. If we consider  $\mathcal{A} = 0$  in the *Minimum Overlapping Area Routing Problem* at  $\alpha = 1.0$  which is the trade off factor (will be explained in later section), i.e. if we consider only the overlapping area as the weight of the link, this condition could be achieved. Therefore, we state the *Minimum Overlapping Area Routing Problem* to be  $\mathcal{NP}$ -complete as it contains the *Region-Disjoint Paths Problem* as an instance. ■

## III. HEURISTIC ALGORITHM

Due to the intractability of this problem, in this section, we propose a heuristic algorithm called the Minimum Overlap Area Routing Algorithm (*MOA*). The algorithm uses the topology aggregation information provided by each domain in order to provision primary and backup paths with a low probability of simultaneous failure. The method for creating these topology aggregations is discussed next.

### A. Topology Aggregation

Due to the privacy restrictions on the exchange of complete domain information with other domains in the network, topology aggregation may be used to exchange limited information about each domain. Typically, topology aggregation provides an aggregated logical topology for each domain, along with some information on the properties of the links in the topology. Common logical topologies used in topology aggregation schemes include: single node, star, and full mesh topologies [8]. In our work, we consider full mesh network topology aggregation, in which border nodes within a domain are connected in full mesh pattern using aggregated links. All the aggregated links between the border nodes are mapped to physical paths in the substrate network. For each aggregated link, the topology aggregation scheme will also provide the distance of the underlying path in the substrate network, but will not provide detailed routing information of the underlying path. We propose to extend the information provided in the topology aggregation to also include information that will assist in finding pairs of paths through a domain that have minimum-area overlapping regions.

In this work, we consider two separate full-mesh topology aggregations for each domain.

1) *Primary Topology Aggregation*: The first topology aggregation maps each aggregated link between two border nodes to the minimum distance path between those border nodes. The total distance of the path is assigned as the weight of the corresponding aggregated link in the topology aggregation. The primary topology aggregation is used to find a minimum-distance primary path in the inter-domain topology. If an aggregated link in the primary aggregated topology is selected for the primary path, we create a *secondary aggregated topology*.

2) *Secondary Topology Aggregation*: In this secondary topology (also a full-mesh topology), each aggregated link is mapped to a path in the domain that has a combination of minimum distance and minimum overlapping area with the path used for the primary path's aggregated link. The approach for calculating a minimum-overlap path is as follows:

**Step 1:** Let  $P'$  represent a set of physical links used in the physical path of the aggregated link selected for the primary path in the domain  $m$ , and let  $P$  represent a set of physical links in the domain  $m$ , that are not in set  $P'$ .

**Step 2:** Calculate the area of the overlapping region of physical link  $e_{(i,j)} \in P$  with the physical links in the primary path,  $P'$ .

**Step 3:** Set the weights of these physical links to  $W_{e_{(i,j)}}$ , considering both the area of the overlapping region and the distance:

$$W_{e_{(i,j)}} = \alpha \times \delta(e_{(i,j)}, \hat{e}_{(i',j')}) + (1 - \alpha) \times \text{dis}(e_{(i,j)}), \quad (9)$$

where  $\alpha$  is a tradeoff parameter between the overlap area and distance.  $\text{dis}(e_{(i,j)})$  is the distance of physical link  $e_{(i,j)}$ , and  $\delta(e_{(i,j)}, \hat{e}_{(i',j')})$  is the area of the overlapping region between physical link  $e_{(i,j)}$  and the physical path for the aggregated link  $\hat{e}_{(i',j')}$  used in the primary path.

Varying the value of parameter  $\alpha$ , allows us to achieve a trade-off between the distance of the secondary path and the

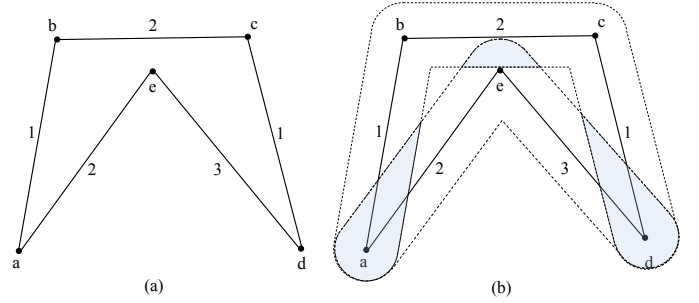


Fig. 5. (a) Primary topology aggregation which is created by selecting the minimum distance path between border nodes within a domain. (b) Secondary topology aggregation which considers the combination of minimum distance and sum of overlapping regions between border nodes within a domain.

area of the overlapping region of the secondary path with the primary path. For lower values of  $\alpha$ , shorter distance paths are selected, and for higher values of  $\alpha$ , paths with less overlapping area are selected.

**Step 4:** Calculate the minimum distance paths between each pair of border nodes in the domain  $m$  using the new metric  $W_{e_{(i,j)}}$ .

The aggregated topology information provided with the secondary aggregated topology includes the distance of the associated paths for each aggregated link and the area of the overlapping region between the path for each aggregated link and the path for the aggregated link used for the primary path, as in Equation 8.

Note: If a domain is not used by the primary path, then its secondary topology aggregation is the same as its primary topology aggregation, and the area of the overlapping region is zero.

*An Example:* Fig. 5 explains the concept of primary topology aggregation and secondary topology aggregation between a pair of border nodes for a given domain. Suppose  $a$  and  $d$  are two border nodes within a domain. For simplicity, let us assume the weights of the links to be the distances between their endpoints. To create the primary topology aggregation (Fig. 5 (a)), we find the minimum distance path between the border nodes  $a$  and  $d$ , i.e. path  $a - b - c - d$ . Now, the aggregated link weight is the distance of the shortest path between the border nodes  $a$  and  $d$  which is 4. Now, suppose that the aggregated link  $\hat{e}_{(a,d)}$  is selected for the primary path in the over-all inter-domain topology. We construct a secondary topology aggregation of this domain by considering paths that minimize a combination of distance and area of the overlapping region with the path used for aggregated link  $\hat{e}_{(a,d)}$  in the primary topology aggregation (shown as gray region in Fig. 5 (b)). The aggregated link weight after the secondary aggregated topology is a linear combination of the path distance and the overlapping area with the primary path.

### B. Path Selection

Once the topology aggregation is provided, we consider the problem of finding two inter-domain paths over the inter-domain topology. To calculate the primary path between a source node and a destination node in the inter-domain

network, we construct an inter-domain topology consisting of the primary aggregated topologies of each domain, with the weight of the aggregated links set as the distance of the underlying paths. We then find the minimum distance path in the inter-domain topology and set this as the primary path.

For the secondary path calculation, we determine the secondary aggregated topologies of each domain based on the aggregated links selected by the primary path in each domain. An inter-domain topology is constructed by combining these secondary aggregated topologies, and the weight of the aggregated links are set to  $\widehat{W}_{\hat{e}(i,j)}$ .

$$\widehat{W}_{\hat{e}(i,j)} = \beta \times \delta(\hat{e}(i,j), \hat{e}(i',j')) + (1 - \beta) \times \text{dis}(\hat{e}(i,j)), \quad (10)$$

where  $\beta$  is the tradeoff parameter between overlap area and distance, similar to  $\alpha$ .  $\delta(\hat{e}(i,j), \hat{e}(i',j'))$  is the area of the overlapping region between the physical path for aggregated link  $\hat{e}(i,j)$  and the physical path for the aggregated link used for the primary path  $\hat{e}(i',j')$ .  $\text{dis}(\hat{e}(i,j))$  is the distance of the physical path for the aggregated link  $\hat{e}(i,j)$ . We then find our backup path based on this new inter-domain topology by calculating minimum distance paths based on  $\widehat{W}_{\hat{e}(i,j)}$  for all aggregated links. We assume that the connection fails if either source or destination is in the disaster area. Solutions involving higher-layer data-backup may be utilized in these cases.

For the case in which the epicenter of the failure is uniformly distributed over the network plane, the probability of simultaneous failure of the primary and backup path is proportional to the overlapping area of the two paths. But when the probability distribution of the failure epicenter has a non uniform distribution, then in this case the weight of the aggregated links are set to be:

$$\widehat{W}_{\hat{e}(i,j)} = \beta \times \gamma(\hat{e}(i,j), \hat{e}(i',j')) + (1 - \beta) \times \text{dis}(\hat{e}(i,j)). \quad (11)$$

### C. Complexity

Let  $V$  be the number of vertices in a domain,  $D$  be the number of domains and  $E$  be the number of edges in a domain. Creating a primary aggregated topology for a domain could be done by using all pair shortest paths for every border node, i.e.  $\mathcal{O}(V^3)$  in the worst case. Finding the primary aggregated topology for all domains would take  $\mathcal{O}(DV^3)$  steps. Finding the primary path over the primary aggregated topologies would take  $\mathcal{O}(E + V \log V)$ , using Dijkstra's algorithm. To create a secondary aggregated topology we consider the domains iterated by the primary path. We first construct vulnerable zones around every edge  $e_{ij} \in E$  within a domain, which takes  $\mathcal{O}(EN^2)$ , where  $N^2$  is number of grid points within a domain. For each grid point we calculate its distance from every edge  $e_{ij} \in E$  to get the overlapping with the primary path, which takes  $\mathcal{O}(EN^2)$  steps. Then we need  $\mathcal{O}(DV^3)$  steps to calculate all pair shortest path based on distance and overlapping area. Thus, creating secondary aggregated topology takes  $\mathcal{O}(DN^2E + DV^3)$ . At last, the secondary path calculation could be done using Dijkstra's algorithm again, i.e.  $\mathcal{O}(E + V \log V)$ , on the secondary aggregated topologies. Thus the overall complexity of this algorithm could be  $\mathcal{O}(DV^3 + DN^2E)$ . Assuming  $D \ll V$ , the complexity is  $\mathcal{O}(V^3 + N^2E)$ .

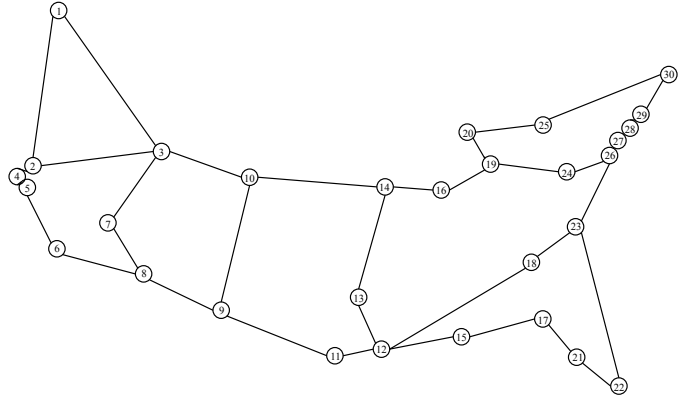


Fig. 6. A 30 node US topology for inter-domain connections.

## IV. NUMERICAL EVALUATION

### A. Network Settings

For numerical evaluation of our approach, we consider a modified version (i.e. nodes are replaced by domains) of a 30 node US topology (Fig. 6) for inter-domain connections [18]. We then consider randomly-generated 10 node topologies for the intra-domain topologies (with a degree of 2-4 for each node). We assume that the area of each domain is  $80 \times 80 \text{ km}^2$ , so that no domains in the network overlap.  $(X, Y)$  coordinates of the 30 inter-domain nodes indicate the location of the center of the domains. Intra-domain coordinates are generated randomly within a network plane within a given distance of the center of the domain. Intra-domain link distances ranges from 50 to 70 kilometers and inter-domain link distances are determined by the coordinates in the 30 node topology, which are much higher than intra-domain link distances. We generate 1000 random source and destination  $(s, d)$  pairs over a fixed network topology, to include  $(s, d)$  pairs with different distance between them. Primary and backup paths are calculated using the aggregated topologies. We ignore the connection if no backup path exists for some  $(s, d)$  pair. We assume parameter  $\alpha = \beta$  for Fig. 7 to Fig. 15. Simulations were also run for cases in which  $\alpha \neq \beta$ , and similar trends were observed.

### B. Experiments and Results

1) *Network with Uniform Distribution of Failure location:* We compare the Minimum Overlap Area Routing Algorithm, denoted by *MOA* in Fig. 7, with Suurballe's Algorithm *SUR* [19], which is used to compute two link disjoint paths between source  $s$  and destination  $d$  over the primary aggregated topologies using only distance information. We also compare the *MOA* algorithm to another heuristic called Full Information Algorithm in which we assume complete domain information is exchanged with other domains, and there is no construction of aggregated topologies. The Full Information Algorithm will select a minimum-distance primary path and will select a backup path with minimum overlapping area from the primary path. We perform this experiment at  $\alpha$  values 0.95, 0.5, and 0.0 for the *MOA* algorithm. Fig. 7 shows that the overlapping area of the primary path and backup path increases with an increase in the radius of failure. As the radius increases,

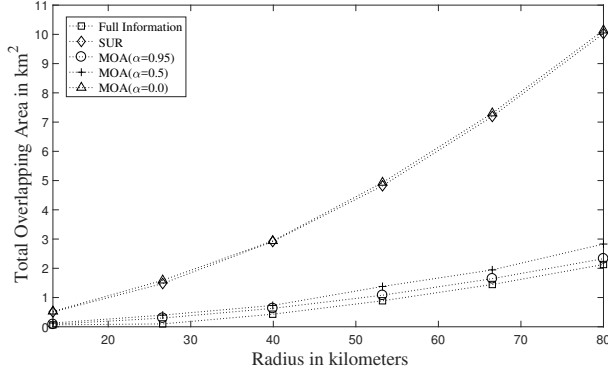


Fig. 7. Total overlapping area of primary and backup path as in Eq. 5 versus the radius of failure in kms, for uniform distribution of the failure epicenter.

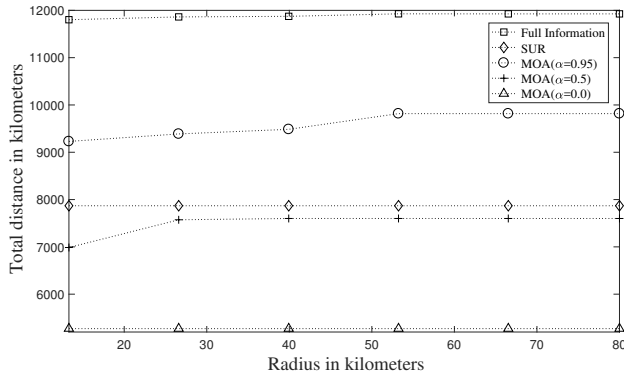


Fig. 8. Total distance of primary and backup path versus radius of failure in kms, for uniform distribution of the failure epicenter.

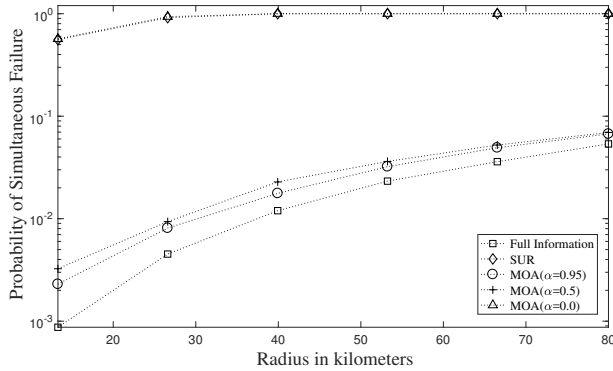


Fig. 9. Probability of simultaneous failure ( $P_A$ ) of primary and backup path versus the radius of failure in kms, for uniform distribution of the failure epicenter.

the  $VZ_{e(i,j)}$  around each edge increases, and thus, finding a completely non-overlapping path becomes difficult. Our results also show that the *MOA* algorithm outperforms the *SUR* algorithm with respect to minimizing the overlapping area and is very comparable to the Full Information solution. In the same experiment, we also compare the overlapping area values of primary and backup paths for different  $\alpha$  values for the *MOA* algorithm. As we increase the value of  $\alpha$ , the overlapping area for primary and backup paths decreases. For  $\alpha = 0$ , the weights of the aggregated links are based only on

the distance, and thus, the total overlapping area is greater.

Next, we compare the three algorithms with respect to the total distance of the resulting paths. In Fig. 8, the total distance for the *SUR* algorithm is constant because it doesn't consider the area of the overlapping region. For the *MOA* algorithm, the distance increases with increase in radius because an increase in radius leads to an increase in  $VZ_{e(i,j)}$  for each link. For the Full Information Algorithm, the distance is the highest because it tries to calculate the most disjoint path from the primary path in the network. We also plot the total distance (i.e. total distance of primary and backup path) for different values of  $\alpha$  as in the previous experiment. For the *MOA* algorithm, the distance increases gradually with increase in radius because an increase in radius leads to an increase in  $VZ_{e(i,j)}$  for each link. For high values of  $\alpha$ , the algorithm gives more preference to disjointness of area rather than minimizing distance, to provide a more survivable pair of paths. Thus, to minimize the total overlapping area, the backup path may traverse a greater number of inter-domain links, resulting in an increase in distance.

For the low values of  $\alpha$ , the algorithm gives more preference to distance effectiveness rather than disjointness. When  $\alpha = 0$ , the total distance does not change with radius because the *MOA* algorithm will only calculate the backup path considering the distance, without considering the overlapping area of the two paths. Also, note that, for  $\alpha = 0.5$  and  $\alpha = 0$ , the total distance of the primary and backup paths is lower than that for the *SUR* algorithm. Since *MOA* doesn't require that the primary and backup paths are completely link-disjoint, the backup path may share some links with the primary path, leading to lower overall distance. In Fig. 9, we obtain probability of simultaneous failure for primary and backup paths for the same set of algorithms as above. We observe an increase in probability of simultaneous failure with the radius, because for the uniform distribution of the location of epicenter, the probability of simultaneous failure is directly proportional to the overlapping area.

For the next experiment, we consider three different intra-domain topologies with 3, 10, and 14 nodes. Intra-domain distances ranges from 50 to 70 kilometers with a degree of 2 to 4 for each node. The inter-domain topology is the same 30 nodes topology [18]. In Fig. 10, we compute the overlapping area between primary and backup paths, for a range of values of  $\alpha$ . We observe that the overlapping area increases as the intra-domain topologies become denser. This happens because in a denser topology, the vulnerable zones around each edge overlap with the vulnerable zones of other edges, and this increases the total overlapping area of two paths. For the same reason, in a denser topology we observe more variation in the overlapping area with the change in  $\alpha$  as compared to sparse topologies. In Fig. 11, we evaluate the total path distance for the *MOA* algorithm in the three topologies. We observe that the total distance increases with the increase in number of intra-domain nodes for each domain. We also observe gradual increase in the total distance for each topology with the radius, for the same reason as mentioned for Fig. 8.

2) *Network with Non-Uniform Distribution of Failure location*: In this section of the evaluation, we obtain the intensity

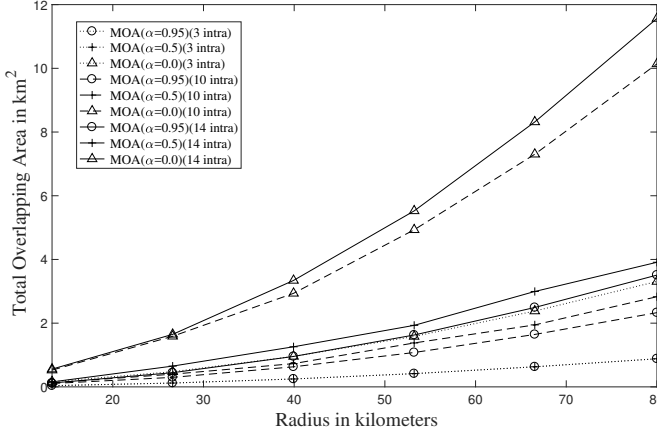


Fig. 10. Total overlapping area comparison for three intra-domain topologies (for  $\alpha = 0.95, 0.5, 0.0$ ) v/s radius in kms.

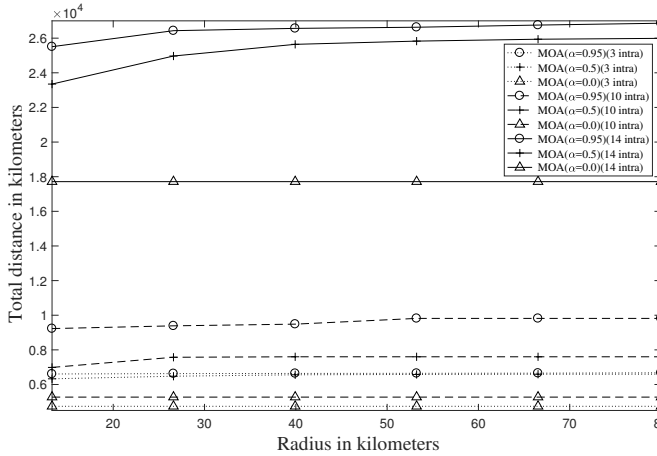


Fig. 11. Total distance comparison for three intra-domain topologies (for  $\alpha = 0.95, 0.5, 0.0$ ) v/s radius in kms.

values of the location coordinates in the network from the hazard map. A way to implement this is to place the coordinates of the 30 node network topology on the map and then normalize the distance between two nodes in terms of pixel distance between their coordinate points.

In the comparison of the Minimum Overlap Area Routing Algorithm, denoted by *MOA* in Fig. 12 and Fig. 13, we observe similar trends compared to the case with uniform distribution of the failure epicenter. The total overlapping area of the primary path and the backup path for *MOA*, *SUR*, and Full Information algorithm increases with an increase in the radius of failure. The total distance for *SUR* is constant, while for the *MOA* algorithm and the Full Information algorithm it increases as before.

Fig. 14 gives a comparison between the probability of simultaneous failure for the three algorithms versus radius for different values of  $\alpha$ . We observe, with an increase in the value of  $\alpha$ , the probability of simultaneous failure decreases. Also there is an increase in the value of probability of simultaneous failure with an increase in radius. For *MOA* at  $\alpha = 0$ , the weights of the aggregated links are based only on the distance,

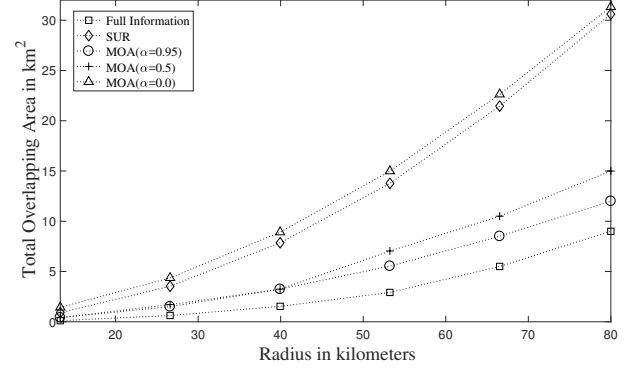


Fig. 12. Total overlapping area of primary and backup path as in Eq. 5 versus the radius of failure in kms, for non-uniform distribution of the failure epicenter.

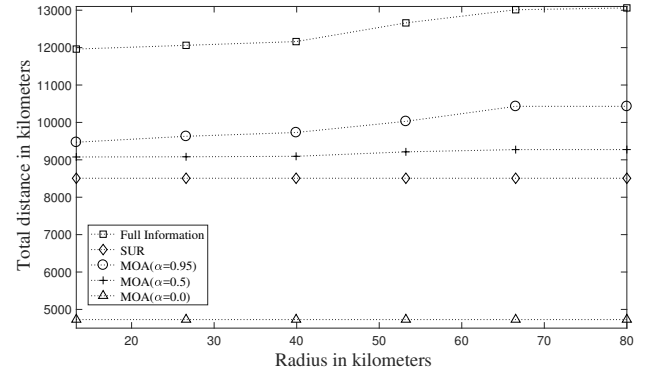


Fig. 13. Total distance of primary and backup path versus radius of failure in kms, for non-uniform distribution of the failure epicenter.

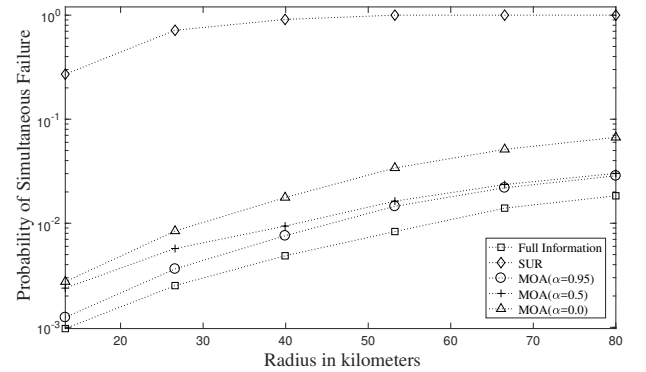


Fig. 14. Probability of simultaneous failure ( $P_A$ ) of primary and backup path versus the radius of failure in kms, for non-uniform distribution of the failure epicenter.

and thus, the probability of simultaneous failure is greater than other values of *MOA* algorithm.

## V. DISCUSSIONS

### A. Modeling of general shaped failure

Our discussion in this work is limited to one circular shape disaster which could occur anywhere in the network plane under both uniform and non-uniform epicenter location. A

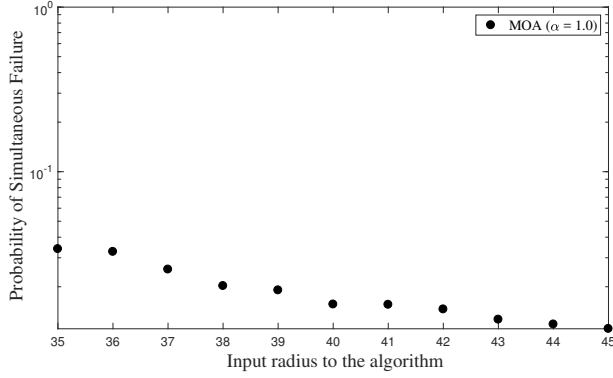


Fig. 15. Probability of Simultaneous Failure when network is designed based on values of the radius that are smaller or larger than the actual failure radius.

more general scenario where the shape of the disaster is not circular may be more difficult to evaluate.

If the shape of the failure is deterministic and known, and if the location of the failure is distributed over the network plane according to density function  $f(x, y)$ , then we can use similar techniques as above to identify the vulnerable zones of each edge and path, and to integrate  $f(x, y)$  over the overlapping vulnerable regions to determine the probability of simultaneous failure.

An alternative approach to deal with general shaped geographic failures is to consider a discrete set of failure events, each with a defined shape. In this case, each failure affects a known set of links, which can be specified as a shared-risk link group, and existing SRLG-based approaches can be used to address the problem.

On the other hand, if the shape of the failure has some random distribution, then the set of affected links cannot be determined by simply considering the location of the epicenter. In this case, for each link or path, one would need to consider the set of all possible failure locations that may potentially impact the link or path, and, for each of these failure locations, determine the probability that the failure will affect the given link or path based on the distribution of the shape of the failure.

### B. Selection of radius for network design

The proposed algorithm assumes a given radius for a failure. If the actual radius of a failure differs from the radius assumed by the algorithm, the cost and robustness of the solution may be affected. In this section, we evaluate the effect of selecting a failure radius that differs from the actual radius of failure. For the experiment in Fig. 15, we select an actual value of failure radius (40 km), and we test for the cases in which the algorithm assumes values of the radius that are smaller or larger than the actual failure radius. If the network design radius is less than the actual radius value, the network will compromise in robustness, i.e. the probability of simultaneous failure will be more. If design radius is more than the actual value of radius, we end up with longer paths, but the probability of simultaneous failure is reduced. Thus, the selection of design radius offers a trade-off between cost and robustness.

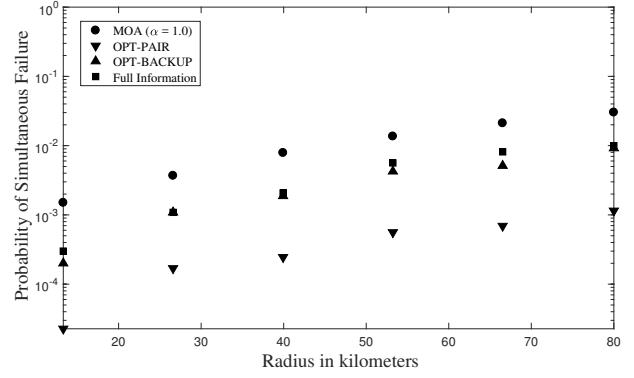


Fig. 16. Probability of Simultaneous Failure for MOA, Full Information, OPT-PAIR, OPT-BACKUP, for a small network.

### C. Tractability for small network size

Although the problem of finding two paths with minimum overlapping area is NP-complete, it may be possible to find an optimal solution to the problem by exhaustively searching over all possible simple paths between a source  $s$  and a destination  $d$ , and selecting the pair of paths that results in the minimum overlap. We refer to this solution as *OPT-PAIR*. Alternatively, if the primary path is given, then the optimal backup path can be found by exhaustively searching over all possible simple paths between  $s$  and  $d$ , and selecting the path that has minimum overlap with the given primary path. This solution is referred to as *OPT-BACKUP*. *OPT-PAIR* and *OPT-BACKUP* can be implemented using a variation of depth first search, resulting in complexity  $\mathcal{O}(EN^2(V!)^2)$  for *OPT-PAIR* and  $\mathcal{O}(EN^2V!)$  for *OPT-BACKUP*, where  $V$  is the number of nodes,  $E$  is the number of edges, and  $N^2$  is the number of grid points.  $EN^2$  is the time to calculate the overlapping area between two paths, and  $V!$  is the worst-case number of simple paths between a pair of nodes. Fig. 16 shows a comparison between the *MOA* algorithm, the Full Information Algorithm, *OPT-PAIR*, and *OPT-BACKUP* in a small graph. We consider a three-domain inter-domain topology with three intra-domain nodes in each domain. *MOA* first calculates the primary path based on the primary aggregated topologies, then it attempts to find a back-up path that has minimum probability of simultaneous failure with the primary path. The Full Information algorithm first calculates the primary path based on the global topology with full information, then attempts to find a backup path with minimum overlap with the primary path over the global topology.

Note that, since *MOA*, Full Information, and *OPT-BACKUP* set the initial primary path based on distance, these solutions have a higher probability of simultaneous failure compared to *OPT-PAIR*, which considers every possible pair of paths. Also, Full Information has performance that is close to that of the *OPT-BACKUP* solution. Thus, most of the gap between *MOA* and the optimal solution is due to the lack of complete information when dealing with multiple domains.

## VI. CONCLUSION

We addressed an important aspect of survivability in multi-domain optical networks with geographically correlated fail-

ures. We formulate probabilistic model based on the non-uniform and uniform probability distribution of the epicenter location. We developed a topology aggregation scheme providing information about geographic distances between links in each domain and use this information to provision primary and backup paths, such that these paths are less likely to fail during the same geographically correlated failure event. We observe that numerical evaluations discussed in this paper indicate the effectiveness of our approach in terms of probability of simultaneous failure and total distance.

#### ACKNOWLEDGMENT

A preliminary version of this work appeared in Proceedings of the IEEE Global Communications Conference (GLOBECOM), Singapore, December, 2017. The authors would like to thank Dr. Ramaswamy Chandrasekaran for his thoughtful contribution towards this work.

#### REFERENCES

- [1] R. Gour, J. Kong, G. Ishigaki, A. Yousefpour, S. Hong, and J. P. Jue, "Survivable routing in multi-domain optical networks with geographically correlated failures," in *GLOBECOM 2017 - 2017 IEEE Global Communications Conference*, pp. 1–6, Dec 2017.
- [2] P. K. Agarwal, A. Efrat, S. K. Ganjugunte, D. Hay, S. Sankararaman, and G. Zussman, "The resilience of wdm networks to probabilistic geographical failures," *IEEE/ACM Transactions on Networking*, vol. 21, pp. 1525–1538, Oct 2013.
- [3] M. Rahnamay-Naeini, J. E. Pezoa, G. Azar, N. Ghani, and M. M. Hayat, "Modeling stochastic correlated failures and their effects on network reliability," in *2011 Proceedings of 20th International Conference on Computer Communications and Networks (ICCCN)*, pp. 1–6, July 2011.
- [4] S. Ramamurthy and B. Mukherjee, "Survivable WDM mesh networks. part I-protection," in *INFOCOM '99. Eighteenth Annual Joint Conference of the IEEE Computer and Communications Societies. Proceedings. IEEE*, vol. 2, pp. 744–751 vol.2, Mar 1999.
- [5] S. Yuan, S. Varma, and J. P. Jue, "Minimum-color path problems for reliability in mesh networks," in *Proceedings IEEE 24th Annual Joint Conference of the IEEE Computer and Communications Societies.*, vol. 4, pp. 2658–2669 vol. 4, March 2005.
- [6] C. Gao, M. M. Hasan, and J. P. Jue, "Domain-disjoint routing based on topology aggregation for survivable multidomain optical networks," *IEEE/OSA Journal of Optical Communications and Networking*, vol. 5, pp. 1382–1390, Dec 2013.
- [7] C. Gao, Y. Zhu, and J. P. Jue, "SRLG-aware topology aggregation for survivable multi-domain optical networks," *IEEE/OSA Journal of Optical Communications and Networking*, vol. 5, pp. 1145–1156, Nov 2013.
- [8] C. Gao, H. C. Cankaya, and J. P. Jue, "Survivable inter-domain routing based on topology aggregation with intra-domain disjointness information in multi-domain optical networks," *IEEE/OSA Journal of Optical Communications and Networking*, vol. 6, pp. 619–628, July 2014.
- [9] H. Drid, B. Cousin, M. Molnar, and S. Lahoud, "A survey of survivability in multi-domain optical networks," *Computer Communications*, vol. 33, no. 8, pp. 1005 – 1012, 2010. Special Section on Hot Topics in Mesh Networking.
- [10] P. Datta and A. K. Somani, "Diverse routing for shared risk resource groups (srrg) failures in wdm optical networks," in *First International Conference on Broadband Networks*, pp. 120–129, Oct 2004.
- [11] F. Xu, N. Min-Allah, S. Khan, and N. Ghani, "Diverse routing in multi-domain optical networks with correlated and probabilistic multi-failures," in *2012 IEEE International Conference on Communications (ICC)*, pp. 6247–6251, June 2012.
- [12] T. Gomes, J. Tapolcai, C. Esposito, D. Hutchison, F. Kuipers, J. Rak, A. de Sousa, A. Iossifides, R. Travanca, J. André, L. Jorge, L. Martins, P. O. Ugalde, A. Pašić, D. Pezaros, S. Jouet, S. Secci, and M. Tornatore, "A survey of strategies for communication networks to protect against large-scale natural disasters," in *2016 8th International Workshop on Resilient Networks Design and Modeling (RNDM)*, pp. 11–22, Sept 2016.
- [13] S. Neumayer and E. Modiano, "Network reliability with geographically correlated failures," in *2010 Proceedings IEEE INFOCOM*, pp. 1–9, March 2010.
- [14] S. Neumayer and E. Modiano, "Network reliability under random circular cuts," in *2011 IEEE Global Telecommunications Conference - GLOBECOM 2011*, pp. 1–6, Dec 2011.
- [15] Snyder, John P., "Map projections: A working manual," 1987. [Online]. Available: <http://pubs.er.usgs.gov/publication/pp1395>.
- [16] (2018,May.)United States Geological Survey, "Seismic hazard maps," 2016. [Online]. Available: <https://earthquake.usgs.gov/hazards/hazmaps/>.
- [17] S. Trajanovski, F. A. Kuipers, A. Ilić, J. Crowcroft, and P. V. Mieghem, "Finding critical regions and region-disjoint paths in a network," *IEEE/ACM Transactions on Networking*, vol. 23, pp. 908–921, June 2015.
- [18] (2017,Sept.)Monarch Network Architects, "Sample optical network topology files," 2016. [Online]. Available: <http://www.monarchna.com/topology.html>.
- [19] J. W. Suurballe and R. E. Tarjan, "A quick method for finding shortest pairs of disjoint paths," *Networks*, vol. 14, no. 2, pp. 325–336, 1984.